Mobility and carrier density in materials with anisotropic conductivity revealed by van der Pauw measurements

O. Bierwagen,* R. Pomraenke, S. Eilers, and W. T. Masselink
Department of Physics, Humboldt-Universität zu Berlin, Newtonstrasse 15, 12439 Berlin, Germany
(Received 10 June 2004; published 12 October 2004)

The validity of four-contact van der Pauw–Hall measurements of rectangularly shaped semiconductors with anisotropic transport properties is investigated analytically, numerically, and experimentally. We show that the carrier concentration is correctly measured using the van der Pauw technique without corrections. Furthermore, the asymmetry in the resistance of the van der Pauw sample is related to the real transport asymmetry through an analytically obtained formula. Thus, the mobility in both principal directions as well as the carrier density can be obtained from van der Pauw data. Measurements of electron concentration and mobility using both the Hall-bar and van der Pauw geometries in semiconductor coupled quantum-wire structures confirm this expectation for different anisotropies.

I. INTRODUCTION

Transport properties of isotropic semiconductors are conveniently measured with the van der Pauw (vdP) method.[1] In contrast to Hall-bar measurements, the vdP technique requires only four sufficiently small contacts placed at the circumference of an arbitrarily shaped (but simply connected) sample. The influence of contact size is taken into account by correction factors.[2] Transport properties of semiconductor nanostructures can be anisotropic due to anisotropic effective masses, structural corrugation in a two-dimensional electron gas (2DEG),[3] the presence of coupled quantum-wires,[4,5] or high Landau-level indices in a two-dimensional electron or hole system.[6,7] The analysis of vdP measurements for anisotropic transport, however, is less than straightforward because the validity of the calculated carrier density is not obvious and the magnitude of anisotropy is overestimated. For example, transport measurements in high Landau levels of a 2DEG show an anisotropy of about 100 in vdP geometry, but only 6 in Hall-bar geometry.[6] In contrast to the vdP geometry, the four-terminal resistances of a Hall-bar geometry directly reflect the actual resistivity in the direction of the bar. A theoretical explanation of this discrepancy is given in Ref. 8, where the relation between anisotropies for both geometries are analytically derived and formulas for the four-terminal resistances are given. These were also experimentally confirmed with structured lateral superlattices.[9] A general solution to the potential problem in an arbitrarily shaped two-dimensional anisotropic medium is given in Ref. 10. With finite-element methods, the effect of a conductivity anisotropy on Hall measurements was numerically calculated for the van der Pauw method and square shaped geometry.[11] (The significant dependence of Hall voltage on anisotropy described in Ref. 11 is not, however, supported by either our numerical calculations or our experimental results.)

The aim of the present paper is to investigate how anisotropic transport properties can be obtained from the results of van der Pauw measurements of a rectangularly shaped sample. In Sec. II, the conductivity tensor describing the anisotropic microscopic (magneto)transport properties of the material is defined, the van der Pauw geometry is presented, and the usual procedure of obtaining isotropic transport parameters from vdP measurements is shown. Within this framework, the four-terminal resistances for given microscopic anisotropies are *analytically* calculated for rectangular samples without magnetic field in Sec. III. Numerical methods allow the calculations to also be extended to include a magnetic field and for given arbitrary shapes. Thus, using finite-element methods, the four-terminal resistances as well as Hall voltages are *numerically* calculated by simulating the experiment. These numerical and analytical results allow carrier concentration and mobility in samples with anisotropic conductivity to be obtained from vdP data. This method is applied to coupled quantum-wire structures with anisotropic transport properties in Sec. IV. The experimental results of both these measurement geometries are compared and discussed in Sec. V to assess the use of van der Pauw measurements for characterizing anisotropic semiconductors.

II. DEFINITIONS

A two-dimensional anisotropic semiconductor without magnetic field is characterized by the conductivity tensor

$$\sigma = \begin{bmatrix} \sigma_{xx} & 0 \\ 0 & \sigma_{yy} \end{bmatrix} \tag{1}$$

with principal conductivities σ_{xx}, σ_{yy} in the mutually perpendicular directions x, y of the two-dimensional (2D) plane. Therefore, the resistivities $\rho_{xx,yy}(\Omega)$ for transport in the principal directions, without magnetic field, can be expressed as

$$\rho_{xx,yy} = \frac{1}{\sigma_{xx,yy}}. \tag{2}$$

Their ratio

$$A = \frac{\rho_{yy}}{\rho_{xx}} = \frac{\sigma_{xx}}{\sigma_{yy}} \tag{3}$$

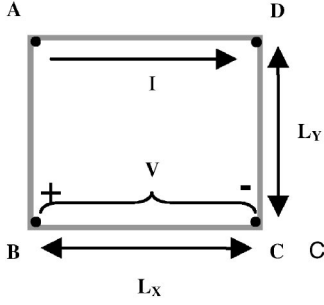is the conductivity anisotropy A.

70 165307-1

FIG. 1. Simple rectangular geometry of size $L_x \times L_y$ with contacts in the corners.

The measured quantities are four-terminal resistances such as

$$R_{AD,BC} \equiv \frac{V_{BC}}{I_{AD}}, \tag{4}$$

with the voltage $V_{BC}(V)$ measured across contacts B and C, and the current $I_{AD}(A)$ flowing through contacts A and D. These resistances depend not only on the resistivity but also on the actual geometry (including contact placement) of the structure. Figure 1 shows the vdP geometry used in the present study as well as by several others.[7,11]

The resistances measured in both transport directions are

$$R_{xx} \equiv R_{AD,BC} \text{ and } R_{yy} \equiv R_{AB,DC}. \tag{5}$$

In isotropic materials, the resistivity ρ fulfills the van der Pauw theorem[1]

$$\exp\left(-\pi\frac{R_{xx}}{\rho}\right) + \exp\left(-\pi\frac{R_{yy}}{\rho}\right) = 1, \tag{6}$$

used to determine the resistivity from experimental data.

In order to determine the carrier density, a magnetic field $B(T)$ perpendicular to the xy plane is applied. Now the conductivity tensor in a magnetic field is

$$\sigma = \frac{Ne}{1 + \mu_x\mu_y B^2}\begin{bmatrix} \mu_x & -\mu_x\mu_y B \\ \mu_x\mu_y B & \mu_y \end{bmatrix}, \tag{7}$$

with homogeneous 2D carrier density $N(m^{-2})$ (negative for electrons) and mobilities $\mu_x, \mu_y(m^2/Vs)$ (negative for electrons) in the principal directions x, y of the 2D plane. Equation (7) ignores the averaging of the individual tensor components over energy. The four-terminal resistance $R_{AC,BD}$ measured with and without magnetic field B results in the Hall coefficient

$$R_H = \frac{R_{AC,BD}(B) - R_{AC,BD}(B=0)}{B}. \tag{8}$$

By symmetry, use of the other diagonal $R_{BD,CA}$ leads to the same Hall coefficient. The carrier density relates to the Hall coefficient by
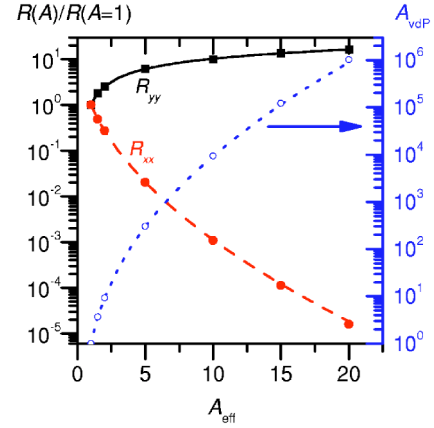

FIG. 2. (Color online) Four-terminal resistances R and their anisotropy A_{vdP} vs effective anisotropy A_{eff}, calculated analytically (lines) and numerically (symbols).

$$N = \frac{r_H}{eR_H} \tag{9}$$

with the Hall scattering factor r_H which depends on the actual scattering processes of both principal transport directions. [In the case of the conductivity tensor defined in Eq. (7), this factor is unity].

III. ANALYTICAL AND NUMERICAL RESULTS

The analytical result for the four-terminal resistance R_{xx} is a function $f(\rho_{xx}, \rho_{yy}, L_x, L_y)$ given in Ref. 8 but for a different geometry. This function is used to calculate[12] R_{xx} for the geometry considered here with the result that

$$\begin{aligned} R_{xx} &= 2f(\rho_{xx}, \rho_{yy}, L_x, 2L_y) \\ &= \frac{8}{\pi}\sqrt{\rho_{xx}\rho_{yy}} \sum_{n=odd^+} \left[n\,\sinh\left(\sqrt{\frac{\rho_{xx}}{\rho_{yy}}\frac{L_y}{L_x}}\pi n\right) \right]^{-1}. \end{aligned} \tag{10}$$

R_{yy} is given by exchanging all x and y in the above equation. For convenience an effective anisotropy

$$A_{eff} = \frac{\rho_{yy}}{\rho_{xx}}\left(\frac{L_x}{L_y}\right)^2 = A\left(\frac{L_x}{L_y}\right)^2 \tag{11}$$

is introduced. A_{eff} takes into account the conductivity anisotropy A and the geometrical aspect ratio of the vdP structure, and is identical to A for square geometry. Using Eqs. (10) and (11), the anisotropy of the four-terminal resistance for rectangular samples is

$$A_{vdP} \equiv \frac{R_{yy}}{R_{xx}} = \frac{\displaystyle\sum_{n=odd^+}\left[n\,\sinh\left(\sqrt{A_{eff}^{-1}}\pi n\right)\right]^{-1}}{\displaystyle\sum_{n=odd^+}\left[n\,\sinh\left(\sqrt{A_{eff}}\pi n\right)\right]^{-1}}. \tag{12}$$

The four-terminal resistances and their anisotropy in our vdP geometry are shown in Fig. 2 for a range of effective anisotropies.

Voltages and resistances can be calculated numerically for arbitrary geometries and arbitrary parameters (material prop-

TABLE I. Numerically calculated Hall coefficients for different conductivity anisotropies at a constant carrier density of $Ne = 1$ C m^{-2}.

A	$R_{AC,BD}(B=0)(\Omega)$	$R_{AC,BD}(B=0.2 \text{ T})(\Omega)$	$R_H(m^2/C)$
1	1×10^{-5}	0.199	0.994
2	0.498	0.697	0.995
10	2.267	2.466	0.994
20	3.569	3.768	0.996
100	9.054	9.250	0.983

erties, B field, external voltages). Specifically, finite-element methods are used to calculate the local electrostatic potential $\Phi(\mathbf{r})$ at the position $\mathbf{r}$ in the 2D plane of the vdP structure. The problem is solved for a rectangle (see Fig. 1) with the magnetoconductivity tensor $\sigma(B)$ defined in Eq. (7). The form of the current density

$$\mathbf{j} = \sigma \mathbf{E} = -\sigma \nabla \Phi(\mathbf{r}), \qquad (13)$$

and the fact that there are no current sources/sinks inside the structure, $\nabla \cdot \mathbf{j} = 0$, results in the elliptic partial differential equation for the potential, $-\nabla \cdot \sigma \nabla \Phi = 0$, to be solved for points inside the structure. Boundary conditions are Neumann type, i.e., no current flows normal to the boundary, at all boundaries except for the bias contacts. The bias contacts are used as source and drain for the current, and mathematically are Dirichlet-type boundaries at *given* constant bias potentials. From the resulting potential distribution, the local current density is calculated according to Eq. (13). Then, integrating the normal current density along a line that divides the sample into two parts, each part containing one bias contact, the total current in the sample is obtained. The four-terminal resistances of the sample are now calculated by dividing the potential difference between the other two contacts (corners) by the current.

For a square ($L_x = L_y$), R_{xx} and R_{yy} were calculated with both methods mentioned above, and R_H was numerically calculated. All calculations were done for different conductivity anisotropies A assuming $\mu_x \geq \mu_y$. For convenience of the numerics, let $Ne = 1$ cm^{-2}, $\sqrt{\mu_x \mu_y} = 1$ m^2/V s, therefore $\mu_x = \sqrt{A}$ m^2/V s, and $\mu_y = 1/\sqrt{A}$ m^2/V s. As bias voltage 1 V is chosen, the magnetic field was set 0.2 T. The following points should be noted: (1) The chosen bias voltage does not influence the calculated four-terminal resistances because all potentials and the current scale linearly with bias; (2) without magnetic field, the chosen scale of mobility and the carrier density do not limit the generality of our considerations as they do not influence the potential distribution; and (3) for the case with magnetic field, different scales of μB lead to the same Hall coefficient R_H. Therefore, the results also apply to more realistic numbers by scaling the mobility or carrier density appropriately. The numerical calculations were done using $\approx 30\,000$ triangles.

The results of the numerical calculation of R_H are given in Table I. The corresponding potential distributions for isotropic and anisotropic ($A = 2$) cases with and without magnetic field are shown in Fig. 3.

We conclude that the Hall voltage as difference between

the case with and without magnetic field is *not* sensitive to the anisotropy. For all anisotropies considered here, the vdP technique correctly determines the carrier density according to Eq. (9). (We find the same result for rectangularly shaped structures.) Our results contradict those of Ref. 11 which (also using finite-element methods) predict considerable variations of R_H even for small anisotropies.

Table II and Fig. 2 display the analytically and numerically calculated results of the four-terminal resistances and their anisotropy.

The numerical results confirm the analytical formula (10) for all anisotropies considered here. For extreme anisotropies ($A = 100$), however, the vdP anisotropy is too high to be practically measured and the accuracy is probably insufficient. We can also verify both methods by putting the resulting four-terminal resistances of the isotropic case ($A = 1$) into the van der Pauw theorem (6) and solving it for ρ. As a result a resistivity of $\rho = 1$ (that we put in as material property) is retrieved, which means that our measurement gives us the correct value. Moreover, in the anisotropic cases, the resistivity ρ obtained from Eq. (6) equals the average resistivity
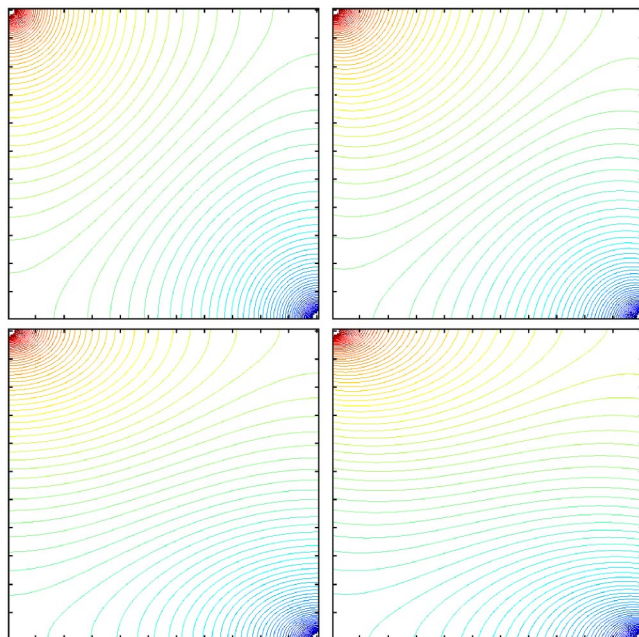

FIG. 3. (Color online) Equivalent-potential distributions in vdP geometry calculated for the same bias current and carrier density. Left column $B=0$, right column $B=0.2$ T, top row $A=1$, bottom row $A=2$. Bias potential is 1 V, 1 div=10 mV.

TABLE II. Four-terminal resistances and their anisotropy A_{vdP} on a square without magnetic field for different conductivity anisotropies A calculated numerically (Num.) and analytically (Analyt.).

A	ρ_{xx}	ρ_{yy}	R_{xx}	(Ω)	R_{yy}	(Ω)	A_{vdP}	$=R_{yy}/R_{xx}$
	(Ω)	(Ω)	Num.	Analyt.	Num.	Analyt.	Num.	Analyt.
1	1	1	0.220	0.221	0.220	0.221	1.00	1.00
1.5	0.817	1.22	0.108	0.109	0.393	0.395	3.64	3.63
2	0.707	1.41	0.0604	0.0599	0.552	0.561	9.13	9.37
5	0.447	2.24	0.00447	0.00453	1.349	1.356	302	299
10	0.316	3.16	2.37×10^{-4}	2.47×10^{-4}	2.21	2.28	9334	9236
15	0.258	3.87	2.45×10^{-5}	2.65×10^{-5}	2.97	2.99	1.21×10^5	1.13×10^5
20	0.224	4.47	3.50×10^{-6}	4.03×10^{-6}	3.57	3.59	1.02×10^6	8.91×10^5
100	0.1	10	1.7×10^{-14}	1.2×10^{-13}	9.05	9.12	5.3×10^{14}	7.9×10^{13}

$$\rho_{ave} = \sqrt{\rho_{xx}\rho_{yy}} \qquad (14)$$

in accordance with theoretical expectations.[10] The numerical calculations showed that, interestingly, the anisotropy of the two-terminal resistances ($R_{AD,AD}$ and $R_{AB,AB}$, i.e., bias voltage divided by total current) strongly underestimates the conductivity anisotropy (1.22, 2.37, and 5.00 for $A=2$, 10, and 100).

The important calculated results are how the conductivity anisotropy is determined from the vdP resistance anisotropy (10) and that the carrier density is correctly measured with the vdP technique.

We determine the principal resistivities from measured four-terminal vdP resistances R_{xx},R_{yy} as follows:

(1) The effective anisotropy A_{eff} is obtained from the anisotropy of measured four-terminal resistances A_{vdP} with the help of Eq. (12).

(2) With known aspect ratio, the conductivity anisotropy A is calculated according to Eq. (11).

(3) Using the van der Pauw theorem (6), the average resistivity $\rho_{ave}=\rho$ is obtained from the measured four-terminal resistances.

(4) The principal resistivities are now calculated from A and ρ_{ave} using Eqs. (3) and (14),

$$\rho_{xx} = \rho_{ave}\sqrt{A}^{-1} \text{ and } \rho_{yy} = \rho_{ave}\sqrt{A}. \qquad (15)$$

Numerically it is shown that the experimentally obtained Hall coefficient R_H [Eq. (8)] *does not* depend on the anisotropy. Therefore, it is used to determine the carrier density the same way as for isotropic materials.

IV. EXPERIMENTAL RESULTS

To test the theoretical results for different anisotropies, samples containing modulation-doped, self-organized, coupled InAs quantum wires in InP (similar to those described in Ref. 5) were grown by gas-source molecular-beam epitaxy. These samples show a temperature-dependent conductivity anisotropy with higher conductivity parallel to the quantum wires. Hall bars (50 μm channel width) for both principal transport directions and square-shaped vdP structures (200 μm edge length) with edges along the principal

transport directions and with contacts in the corners (see Fig. 1) were prepared on the *same* piece of sample by electron-beam lithography and shallow mesa etching. Thus, it is ensured that both Hall-bar and vdP structures have the same microscopic transport properties and can be readily compared.

Transport measurements were performed with these structures at the same time in a temperature range of 10–320 K thus varying the conductivity anisotropy. A constant dc bias current of 1 μA was chosen as a trade-off between minimizing sample heating and maintaining measurement accuracy. Hall coefficients were measured in a magnetic field of 0.5 T. For the Hall-bar case, the Hall coefficient was measured in the Hall bar along the low-mobility direction. In a separate measurement (not shown here) the Hall coefficients were simultaneously measured in Hall bars along both principal directions. They agree within an uncertainty of ±3%.

The resistivities $\rho_{xx,yy}$ and two-dimensional carrier density N were calculated from the data of the vdP measurements (as described in the preceding section) and the Hall-bar measurements separately. The results are given in Figs. 4 and 5. The anisotropies A and A_{vdP} from Hall-bar and vdP measurement range from 2.4 to 6.6 and 12 to 794, respectively.

V. DISCUSSION

Despite a change of anisotropy by a factor of almost 3, the measured carrier density N (Fig. 4) varies only slightly. This variation of N is considered to be independent of the anisotropy. Moreover, for the entire anisotropy range, the carrier density obtained by vdP measurement agrees very well with the Hall-bar result, confirming our analytically obtained results. Both measurement methods are equally good to determine the Hall coefficient, also in anisotropic media.

The average resistivity ρ_{ave} from the Hall-bar results agrees well with the result ρ from the vdP measurement (Fig. 5).

With the vdP method, the quantities N and ρ measured so far can be correctly obtained. This holds true even for arbitrary geometries.[10] In contrast, the anisotropy of four-terminal resistances depends also on the particular geometry, even more crucially than on the conductivity anisotropy as
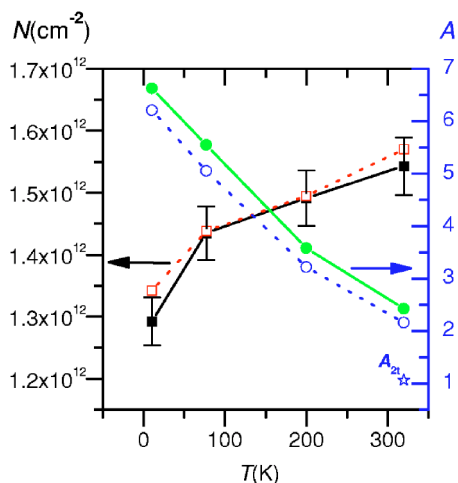
FIG. 4. (Color online) Conductivity anisotropy A and carrier density N obtained from Hall-bar measurements (solid symbols, solid lines) and van der Pauw measurements (open symbols, dotted lines) at different temperatures. The data point A_{2t} is the anisotropy of the two-terminal resistance of the vdP measurement. The error bars of N visualize a relative error of $\pm 3\%$. The lines are to guide the eye.

discussed later. In our experiment the geometry was very precisely defined using lithography. Figure 4 shows a quite good agreement of the anisotropies but not as well as the other quantities. This also affects the calculated principal resistivities (see Fig. 5) because they are calculated with the anisotropy and the average resistivity. A possible reason for the deviation is the four-terminal resistance in the high-mobility direction (see R_{xx} in Fig. 2), which drops quickly with increasing anisotropies. This makes precise measurements more difficult and is regarded as the limiting factor of accuracy in our experiment. For more complex (nonrectangular) geometries, finite-element methods, as presented here, can be used to numerically calculate a relation between conductivity anisotropy and anisotropy of four-terminal resistances to substitute Eq. (12).
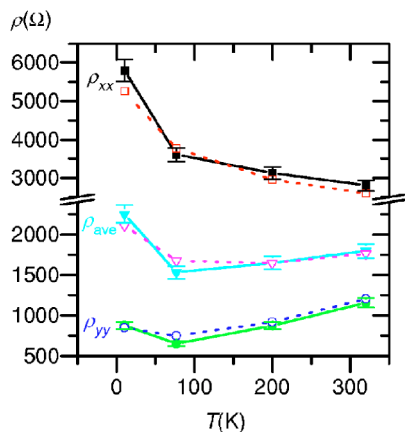

FIG. 5. (Color online) Resistivities of both principal directions and average resistivity obtained from Hall-bar measurements (solid symbols, solid lines) and van der Pauw measurements (open symbols, dotted lines) at different temperatures. The error bars visualize a relative error of $\pm 5\%$. The lines are to guide the eye.

Special care has to be taken of the geometry in order to measure the conductivity anisotropy accurately. In Eq. (11) this is obvious with the $(L_y/L_x)^2$ factor as opposed to ρ_{xx}/ρ_{yy}. The Hall-bar geometry is more forgiving as the relevant lengths (channel width, distance of the voltage probes) just like the conductivity anisotropy, enter linearly into the anisotropy of the four-terminal resistances. The geometry consists of the contacts and the shape of the transport structure. The contacts have to be at the edge of the structure as a precondition for vdP measurements, the position must be well defined (e.g., in the corners of the rectangle), and the contacts should be as small as possible. The size of the contacts is an additional uncertainty to the effective contact position because it is not necessarily known which part of the contact microscopically reaches the conducting layer in the alloying process. With lithography, contacts can be made small and placed outside the vdP structure such as voltage probes of a Hall bar.

Using a *rectangular* geometry $(L_x \neq L_y)$ can help us to increase the measurement accuracy of the vdP anisotropy substantially by tuning the effective anisotropy A_{eff} closer to unity. For example, a conductivity anisotropy range of $1 \leq A_1 < A < A_2$ can be turned into an effective anisotropy range of $1/\sqrt{A_1 A_2} < A_{\mathrm{eff}} < \sqrt{A_1 A_2}$ by using an aspect ratio of $L_x/L_y = \sqrt[4]{A_1 A_2}$.

There are also general disadvantages of the vdP method compared to the Hall-bar method. The failure of one contact renders the vdP structure unusable. Also, macroscopic defects can disturb the current paths in the vdP structure, thus drastically changing the effective geometrical anisotropy. The vdP method cannot discriminate this effect against the conductivity anisotropy. On the other hand, Hall bars with multiple voltage probes for each transport direction can help us to find out problems with macroscopic defects, and alternative contacts can be used in case of a contact failure.

VI. CONCLUSION

To conclude, we have described in detail how to accurately characterize rectangularly shaped structures with anisotropic conductivity using van der Pauw–Hall measurements. An analytical correction is presented to obtain the anisotropy of the conductivity from the measured resistances. It was further shown through a numerical calculation that the Hall coefficient is, in fact, correctly obtained from the vdP data. Combining these two results, the vdP data can be used to obtain the sheet carrier concentration as well as the mobilities in the two principal directions. This anisotropic correction technique was tested on coupled quantum-wire structures with temperature-dependent anisotropy. For all investigated anisotropies, the corrected vdP results agree with those measured using Hall-bar structures. Thus, over a wide range of anisotropies, the corrected vdP technique is an accurate and convenient alternative to the Hall-bar geometry.

*Electronic address: bierwagen@physik.hu-berlin.de

[1] L. T. van der Pauw, Philips Res. Rep. **13**, 1 (1958).

[2] P. Blood and J. W. Orton, *The Electrical Characterization Of Semiconductors: Majority Carriers And Electron States*, edited by N. H. March, Techniques of Physics Vol. 14, (Academic Press, 1992), p. 21.

[3] K.-J. Friedland, R. Hey, O. Bierwagen, H. Kostial, Y. Hirayama, and K. H. Ploog, Physica E (Amsterdam) **13**, 642 (2002).

[4] C. Walther, W. Hoerstel, H. Niehus, J. Erxmeyer, and W. T. Masselink, J. Cryst. Growth **209**, 572 (2000).

[5] O. Bierwagen, C. Walther, W. T. Masselink, and K.-J. Friedland, Phys. Rev. B **67**, 195331 (2003).

[6] M. P. Lilly, K. B. Cooper, J. P. Eisenstein, L. N. Pfeiffer, and K. W. West, Phys. Rev. Lett. **82**, 394 (1999).

[7] M. Shayegan, H. C. Manoharan, S. J. Papadakis, and E. P. De Poortere, Physica E (Amsterdam) **6**, 40 (2000).

[8] S. H. Simon, Phys. Rev. Lett. **83**, 4223 (1999).

[9] A. Endo and Y. Iye, J. Phys. Soc. Jpn. **71**, 2067 (2002).

[10] H. Shibata and R. Terakado, J. Appl. Phys. **66**, 4603 (1989).

[11] Y. Sato and S. Sato, Jpn. J. Appl. Phys., Part 1 **40**, 4256 (2001).

[12] The geometry used in Refs. 6, 8, and 9, is also rectangular but with the current contacts placed in the center of opposite edges. The voltage is measured in the corners. Splitting this rectangle of dimension $L_x \times L_y$ along the connection of the current contacts, we obtain two rectangles of our geometry (all contacts in the corners) with dimensions $L_x \times 1/2 L_y$ each with the same potential distribution, half the total current, and therefore twice the resistance of the former structure.